

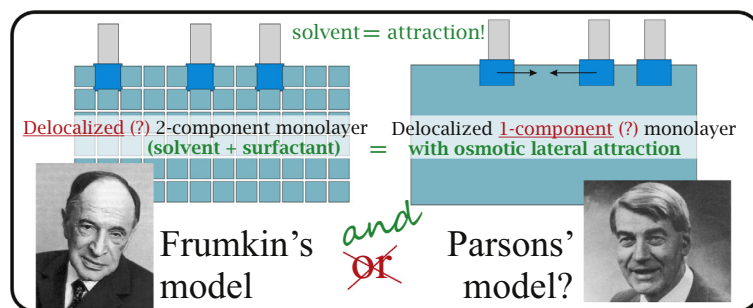
# Effective osmotic cohesion due to the solvent molecules in a delocalized adsorbed monolayer

Radomir I. Slavchov<sup>a,\*</sup>, Ivan B. Ivanov<sup>b</sup>

<sup>a</sup>Department of Chemical Engineering, University of Cambridge, West Site, Philippa Fawcett Drive, Cambridge CB3 0AS, United Kingdom

<sup>b</sup>Laboratory of Chemical Physics and Engineering, Faculty of Chemistry and Pharmacy, Sofia University, 1 J. Bourchier, 1164 Sofia, Bulgaria

## GRAPHICAL ABSTRACT



## ARTICLE INFO

### Article history:

Received 9 July 2018

Revised 8 August 2018

Accepted 9 August 2018

Available online 10 August 2018

### Keywords:

Adsorption

Liquid interface

Osmotic effect

Cohesion

Lateral depletion force

Monolayer

Non-ionic surfactant

Ethylene glycol monoalkyl ethers

Alcohols

## ABSTRACT

A molecular thermodynamic model is derived for an uncharged delocalized surfactant monolayer adsorbed at a liquid interface, taking explicit account for the solvent molecules present in the monolayer. The model is based on the scaled particle theory of hard-disc mixtures, and is also extended to sticky discs (i.e. attraction between the adsorbed molecules). Upon compression of the adsorbed layer, the solvent is expelled from it. The respective osmotic effect on the equation of state is shown to be equivalent to an effective lateral depletion attraction between the surfactant molecules. This effective osmotic cohesion causes an increase of the value of the attraction parameter  $\beta$  of the monolayer. The smaller the size of the surfactant polar head group is, the larger the effective attraction the model predicts. This trend is verified with data for the adsorption at water|air surface of alcohols, undissociated acids, and hexaethylenglycol monoalkyl ethers. The proposed theory allows the amount of solvent in the monolayer to be estimated, which is shown to be important for the neutron reflectivity of the surface.

© 2018 Elsevier Inc. All rights reserved.

## 1. Introduction<sup>1</sup>

Half a century has passed since the famous scientific “battle” between Frumkin and his collaborators, and Parsons, Buff and

\* Corresponding author.

E-mail address: [ris26@cam.ac.uk](mailto:ris26@cam.ac.uk) (R.I. Slavchov).

<sup>1</sup> Days before the completion of this work, Professor Ivan B. Ivanov (1935–2018) has sadly passed away. His relentless passion for knowledge, eloquence, and strength of character will always be an example to follow for me.

Stillinger. The battlefield was the theory of adsorption [1]. Parsons, Buff and Stillinger [2–4] argued that a site model such as Langmuir's cannot provide a satisfactory description for the strictly *delocalized* adsorption of ions at the water|mercury interface; they have championed instead the theory of two dimensional (2D) hard-disc liquids and a nearly exact equation of state (EoS) due to Helfand, Frisch, and Lebowitz [5] (HFL). In response, Frumkin [1,6] reminded that the Langmuir equation, when applied to adsorption of ions from aqueous solution, is not merely a surface

site model – it is a direct consequence of the lattice (Flory-Huggins) theory for a mixture of water and ions. Frumkin further pointed out that a single component EoS such as HFL, with its complete neglect of the water molecules, is no sounder than the Langmuir model. The response of Parsons – then a young man having a great respect for his senior colleague [7] – to Frumkin's criticism was half-hearted [8].

The Langmuir model and its derivatives still dominate the adsorption literature [9–15]. Significantly, Parsons himself was not persistent in pursuing a delocalized description of the adsorbed layer and, in his later works, he developed localized models for liquid interfaces, e.g., [16]. This might seem as a victory for Frumkin, but Frumkin himself was not too convinced either, stating that his arguments “cannot serve, of course, as a sufficient theoretical basis for the application of Langmuir's equation to real systems. . . but it seems to me that these arguments can help when choosing the direction for the further development of the theory of adsorption at the surface of solutions” [6]. Occasionally, variants of the HFL EoS are used for surfactant monolayers [17–24], and indeed have clear advantages. In fact, the application of the Langmuir model (or its extensions to cohesive monolayers, such as Frumkin's model) to surfactant films adsorbed at liquid interfaces leads to several paradoxes which can be traced back to the delocalized nature of the monolayer [24]:

- (i) the Langmuir model's area per molecule determined from adsorption data is as much as twice as large as the crystallographic one, while, in theory, the two quantities should have similar values.
- (ii) The area parameter of Langmuir's model is not transferable from one type of interface to another – to fit the experimental data, one has to use one area of the surfactant for water|air (W|A) and another for water|oil interfaces.
- (iii) Frumkin's model [25] (localized EoS with attraction) modifies Langmuir's to account for 1st neighbours' attraction via the lateral attraction parameter  $\beta$ . When applied to adsorption data for surfactants at water|oil interfaces, this model yields unphysical negative values of  $\beta$ , a paradox that disappears when Parsons' model (delocalized EoS with attraction) is used instead – the expected small positive  $\beta$  are obtained with it.

In any case, the advantage of this or the other model when compared to experimental data does not change the fact that both sides in the dispute were most definitely correct: the Langmuir model and the lattice theory of adsorption provide a description of the adsorption layer that is localized, which is not realistic for liquid interfaces; and, indeed, the HFL model is unconvincing for it neglects completely the solvent molecules at the surface (while the amount of solvent in the monolayer is essential for its properties, e.g., Ref. [26]).

The aim of this work is to resolve the dispute by providing a description that is both delocalized and accounts for the solvent. In other words, we propose a theory of the osmotic effect due to the solvent molecules present in a monolayer adsorbed at a liquid interface (delocalized adsorption) on the thermodynamic properties of this monolayer. In Section 2.2, we analyse the theory of a 2-component hard-disc mixture (direct attraction neglected) and we show that the presence of solvent in the monolayer results in effective osmotic cohesion of it (2D lateral depletion attraction between the surfactant head groups). In Section 2.3, we simplify the results for hard-disc mixture by making use of the concept for osmotic cohesion, and in Sections 2.3 and 3, we generalize it to strongly cohesive (attractive) surfactant molecules. The new model so-obtained is a natural theoretical approach to adsorption of non-ionic amphiphiles at liquid interfaces. We demonstrate the feasibility of the model by comparing it to data for the adsorption

at water|air of 3 homologous series of surfactants of different hard-disc area of the polar head group: alcohols, non-dissociated acids and hexaethyleneglycol monoalkyl ethers (Section 3).

The terminology we use in this manuscript is standard for the field of statistical and chemical thermodynamics (localized, delocalized, osmotic effect, depletion force), but for the ease of readers of other backgrounds and to avoid confusion, we provide a description in the supplementary material S1; there, a list of symbols and abbreviations is also given.

Supplementary data associated with this article can be found, in the online version, at <https://doi.org/10.1016/j.jcis.2018.08.025>.

## 2. Theory

### 2.1. Single-component hard-disc liquid

Before approaching the problem of two-component monolayers, we will briefly review the theory of delocalized single-component hard-disc 2D fluid. Helfand, Frisch and Lebowitz derived an almost exact surface EoS for delocalized adsorption layer of hard discs in the absence of attraction, by using the apparatus of the scaled particle theory [5]:

$$\frac{\alpha_s \pi^S}{k_B T} = \frac{\psi_s}{(1 - \psi_s)^2}. \quad (1)$$

Here,  $\pi^S$  is the surface pressure of the monolayer,  $\pi^S \equiv \sigma_0 - \sigma$ ;  $\sigma$  is surface tension;  $\sigma_0$  is surface tension of the neat surface (at  $\psi_s = 0$ );  $\psi_s \equiv \alpha_s \Gamma_s$  is the surface fraction covered by surfactant;  $\Gamma_s$  is adsorption of surfactant;  $\alpha_s$  is the hard-disc area of the surfactant molecule. The HFL model has been found to agree excellently with data for monolayers of both ionic and non-ionic surfactants at water|oil interfaces [23,24], where other popular models lead to unreasonable adsorption parameters. The hard-disc (repulsion only) HFL model is not suitable for W|A, as at this interface there exists a significant lateral van der Waals attraction between the adsorbed molecules. Parsons [3] generalized the HFL EoS (1) to attractive molecules by adding to it a binary interaction term,  $\beta \psi_s^2$ , to obtain an EoS that has been reinvented many times [17,20]:

$$\frac{\alpha_s \pi^S}{k_B T} = \frac{\psi_s}{(1 - \psi_s)^2} - \beta \psi_s^2; \quad (2)$$

here,  $\beta$  is the so-called lateral attraction parameter. The attraction term in Eq. (2) is semi-empirical; in result, the model is unsatisfactory at high  $\psi_s$  and large values of  $\beta$  [24]. A more reliable EoS for attractive molecules is offered by the sticky disc (SD) model of Ivanov et al. [21–24]:

$$\frac{\alpha_s \pi^S}{k_B T} = \frac{R_\beta - 1}{2\beta(1 - \psi_s)}, \quad \text{where} \quad R_\beta = \sqrt{1 + 4\beta \frac{\psi_s}{1 - \psi_s}}. \quad (3)$$

The corresponding SD surface activity coefficient  $\gamma_s$  follows from the Gibbs isotherm,  $d(\alpha_s \pi^S / k_B T) = \psi_s d(\ln \gamma_s \psi_s)$ , as:

$$\ln \gamma_s = -\ln(1 - \psi_s) + \left(2 + \frac{1}{\beta}\right) \ln \frac{2}{1 + R_\beta} + \frac{\psi_s(4 - 3\psi_s)}{(1 - \psi_s)^2} \frac{2}{1 + R_\beta}. \quad (4)$$

The respective adsorption isotherm (the chemical equilibrium condition for the surfactant at the surface and in the bulk) of the SD model reads

$$\alpha_s K_a C_s = \gamma_s \psi_s, \quad (5)$$

where  $K_a$  [m] is the adsorption constant ( $RT \ln K_a$  is the standard adsorption free energy) and  $C_s$  [ $\text{m}^{-3}$ ] is the concentration of the surfactant [24].

An important feature of the EoS (2) and (3) is that they, unlike all other popular adsorption models, agree with the theoretically expected virial expansion [24]:

$$\frac{\alpha_s \pi^S}{k_B T} \xrightarrow{\psi_s \rightarrow 0} \psi_s + \frac{B_2}{\alpha_s} \psi_s^2 + \dots, \quad \text{with 2}^{\text{nd}} \text{ virial coefficient } B_2 = 2\alpha_s - \alpha_s \beta. \quad (6)$$

The  $2\alpha_s$  term in Eq. (6) is the repulsive hard-disc part of the surface virial coefficient  $B_2$ , and  $-\alpha_s \beta$  is its attractive part. For 1-component liquid made of hard discs that attract to each other,  $\beta$  can be computed from the binary attraction potential  $u_{\text{attr}}(\rho)$  as [19,20]

$$\beta = \frac{1}{R_s^2} \int_{2R_s}^{\infty} (e^{-u_{\text{attr}}(\rho)/k_B T} - 1) \rho d\rho, \quad (7)$$

where  $R_s$  is the hard-disc radius of the surfactant ( $\alpha_s = \pi R_s^2$ ), and  $\rho$  is distance between the interacting molecules. A simple expression for  $u_{\text{attr}}$  at W/A was proposed in Refs. [20,27] – two adsorbed surfactant molecules of straight hydrocarbon chains separated by a distance  $\rho$  experience van der Waals attraction between each other of potential

$$u_{\text{attr}}(\rho) = -\frac{nL_{\text{CH}_2}}{4l_{\text{CH}_2}\rho^5} \left( 3\arctan \frac{nl_{\text{CH}_2}}{\rho} + \frac{nl_{\text{CH}_2}\rho}{\rho^2 + n^2 l_{\text{CH}_2}^2} \right); \quad (8)$$

here,  $n$  is the number of methylene ( $\text{CH}_2$ ) groups in the hydrocarbon chain assumed to stick above the aqueous phase (those that remain immersed in water should contribute negligibly to the van der Waals attraction);  $L_{\text{CH}_2} = 4.24 \times 10^{-78} \text{ m}^6 \text{ J}$  is the London constant for the interaction between two  $\text{CH}_2$  groups, and  $l_{\text{CH}_2} = 1.26 \text{ \AA}$  is the length of a  $\text{CH}_2$  group along the hydrophobic chain [28]. The SD model (3)–(5), with  $\beta$  computed via Eqs. (7) and (8), has been found to agree very well with surface tension data for many cohesive monolayers at W/A [24]. However, just as HFL, the SD model does not account explicitly for the presence of solvent molecules in the plane of the monolayer, which makes Frumkin's criticism relevant [1], as outlined in the introduction.

## 2.2. A hard-disc liquid mixture

Let the polar head groups of the adsorbed surfactant molecules be located in a 1-molecule thick surface layer containing solvent, as schematized in Fig. 1. The justification for this *monolayer model* has been given by Defay and Prigogine, *sec. XI.6* of Ref. [29]: the density drop in a surface layer indeed occurs within a distance of the order of 1–2 molecular diameters, unless the system is close to a critical point. The surface layer in the absence of surfactant is known to be of decreased density in comparison with the bulk fluid – let this surface density correspond to a certain surface coverage of  $\psi_{w0}$  with solvent molecules. The adsorption of surfactant (covering a fraction  $\psi_s$  of the surface) is expected to expulse the solvent from the surface layer, i.e. in the presence of surfactant, the solvent's  $\psi_w$  must be smaller than  $\psi_{w0}$ .

The surface layer is further assumed to behave as a mixture of hard discs of different areas, thus upgrading the HFL model to account for the solvent present at the surface (or alternatively, upgrading Frumkin's formulation of the Langmuir model in Refs. [1,6] to make it delocalized). The EoS predicted by the scaled particle theory for a hard-disc mixture has been derived by Lebowitz, Helfand and Praestgaard (LHP) [30]; for a binary mixture, their eq 6.7 can be written as

$$\frac{\alpha_s \pi^S}{k_B T} = \frac{\psi_s + r\psi_w - (\sqrt{r} - 1)^2 \psi_w \psi_s}{(1 - \psi_s - \psi_w)^2} - \frac{r\psi_{w0}}{(1 - \psi_{w0})^2}; \quad (9)$$

here,  $\psi_w \equiv \alpha_w \Gamma_w$  is the surface fraction covered by solvent (water) molecules;  $\Gamma_w$  is the surface density of solvent molecules in the plane of the monolayer (its relation to the Gibbs adsorption is discussed in the supplement S1);  $\alpha_w$  is the hard-disc area of a solvent molecule;  $\psi_{w0} = \alpha_w \Gamma_{w0}$ , where  $\Gamma_{w0}$  is the surface density of solvent molecules at the neat surface;  $r \equiv \alpha_s / \alpha_w$  is the surfactant/solvent hard-disc area ratio. The Gibbs fundamental isotherm relates this EoS to the chemical potentials (or equivalently, to the surface activity coefficients  $\gamma_s$  and  $\gamma_w$ ) of the two components:

$$d \frac{\alpha_s \pi^S}{k_B T} = r\psi_w d(\ln \gamma_w \psi_w) + \psi_s d(\ln \gamma_s \psi_s). \quad (10)$$

The position of the Gibbs equimolecular surface that corresponds to this model is analysed in the supplement S1. For a binary mixture, both  $\gamma_s$  and  $\gamma_w$  can be derived from Eq. (10); schematic of the derivation is given in S5. The final result reads:

$$\begin{aligned} \ln \gamma_w &= -\ln(1 - \psi_s - \psi_w) \\ &+ \frac{\psi_w(3 - 2\psi_w) + \psi_s \left[ \frac{2}{\sqrt{r}}(1 - \psi_s) + \frac{1 - \psi_w}{r} - 3\psi_w \right]}{(1 - \psi_s - \psi_w)^2}; \\ \ln \gamma_s &= -\ln(1 - \psi_s - \psi_w) \\ &+ \frac{\psi_s(3 - 2\psi_s) + \psi_w \left[ 2\sqrt{r}(1 - \psi_w) + r(1 - \psi_s) - 3\psi_s \right]}{(1 - \psi_s - \psi_w)^2}. \end{aligned} \quad (11)$$

These activity coefficients correspond to a standard state of infinitely dilute (“empty”) monolayer, i.e.  $\gamma_w = \gamma_s = 1$  when  $\psi_w = \psi_s = 0$ ; this is in contrast to Eq. (4), which involves the implicit assumption that  $\gamma_s = 1$  when  $\psi_s = 0$  and  $\psi_w = \psi_{w0}$  – i.e. the standard state there is the neat surface. The new empty monolayer standard state requires a different general form of the adsorption isotherm for the surfactant – instead of Eq. (5), one has to use

$$\alpha_s K_a C_s = \gamma_s \psi_s / \gamma_{s0}, \quad (12)$$

where  $\gamma_{s0} = \gamma_s(\psi_s = 0, \psi_w = \psi_{w0})$  is the activity of the surfactant at the neat surface, in a monolayer dilute with respect to the surfactant only (but not with respect to the solvent).

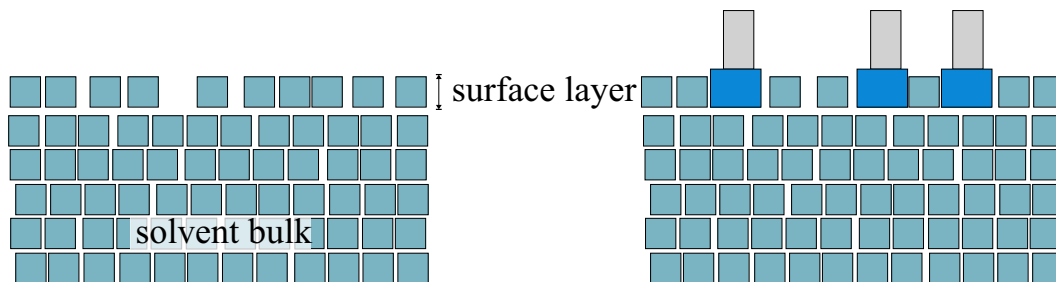


Fig. 1. Schematic of the model: structure of the surface layer before and after the adsorption of surfactant.

Equations equivalent to (9) and (11) have been used by Nikas et al. [19] to model mixed adsorption layer of two non-ionic surfactants (still neglecting the penetration of solvent in the monolayer). Fraser et al. [31] used equivalent formulation to analyse the case of a surfactant with internal degrees of freedom that can assume two spatial arrangements at the surface, of different hard-disc areas and adsorption energies (but again neglecting the solvent).

The amount of water  $\psi_w$  in the surface layer decreases with the increase of the adsorption  $\Gamma_s$  of surfactant. However, if the bulk surfactant solution is dilute, then, to a good approximation, water is of constant chemical potential independent of the amount of dissolved surfactant (the case of concentrated solutions is considered briefly in S4). The dependence of  $\psi_w$  on  $\psi_s$  at constant chemical potential of the solvent follows from the equilibrium condition  $\gamma_w - \psi_w = \gamma_{w0} \psi_{w0}$  (i.e. the activity of the solvent in the monolayer is equal to that of solvent at the neat surface as both are equal to the bulk activity of the solvent); here, the subscript 0 again indicates neat water surface ( $\gamma_{w0}$  is  $\gamma_w$  at  $\psi_s = 0$ ). This condition, together with the first of Eqs. (11), leads to the adsorption isotherm of the solvent:

$$\frac{\psi_w}{1 - \psi_s - \psi_w} e^{\frac{\psi_w(3-2\psi_w) + \psi_s \left[ \frac{2\sqrt{r}(1-\psi_s)}{\sqrt{r}(1-\psi_s)} + \frac{1-\psi_w}{r} - 3\psi_w \right]}{(1-\psi_s-\psi_w)^2}} = \frac{\psi_{w0}}{1 - \psi_{w0}} e^{\frac{\psi_{w0}(3-2\psi_{w0})}{(1-\psi_{w0})^2}}. \quad (13)$$

The adsorption isotherm of the surfactant is obtained by substituting the surface activity coefficient  $\gamma_s$ , Eq. (11), into Eq. (12):

$$\alpha_s K_a C_s = \frac{\psi_s(1 - \psi_{w0})}{1 - \psi_s - \psi_w} e^{\frac{\psi_s(3-2\psi_s) + \psi_w[2\sqrt{r}(1-\psi_w) + r(1-\psi_s) - 3\psi_s]}{(1-\psi_s-\psi_w)^2}} \frac{\psi_{w0}[2\sqrt{r}(1-\psi_{w0}) + r]}{(1-\psi_{w0})^2}. \quad (14)$$

The two adsorption isotherms (13) and (14), together with the LHP EoS (9), completely define the state of the surface (i.e.  $\pi^S$ ,  $\psi_w$ , and  $\psi_s$  are defined as functions of  $C_s$ ), if the hard-disc areas  $\alpha_s$  of the surfactant and  $\alpha_w$  of the solvent, and the neat surface density  $\psi_{w0}$  are known. In the limit of dry monolayer ( $\psi_w \rightarrow 0$ ), the isotherm of the surfactant simplifies to the one following from the HFL model, cf. S3.

The van der Waals radius of a water molecule is 1.39 Å, which corresponds to hard-disc area of  $\alpha_w = 6.07 \text{ \AA}^2$  and hard-sphere volume  $v_w = 11.25 \text{ \AA}^3$ . The molecular volume (molar volume divided by Avogadro's number) of pure water at 25 °C is  $V_w = 30.01 \text{ \AA}^3$ . Assuming that the density of the surface layer is similar to that of the bulk, one can estimate the molecular area of the neat surface at  $A_w = V_w^{2/3} = 9.66 \text{ \AA}^2$ , which corresponds to a coverage of the neat surface of  $\psi_{w0} = \alpha_w/A_w = 0.63$ . However, the surface layer is well-known to be of decreased density (e.g., sec. XI.6 of Ref. [29]). A measure of this decrease is the so-called “hydrophobic gap” width: the X-ray reflectivity of the interface between water and a hydrophobic material has been shown to be the same as if a vacuum gap of thickness 1.4 Å [32] existed between two bulk phases, aqueous and hydrophobic, of normal density. This shows that the density of the surface layer of water (that is  $\sim 2.8 \text{ \AA}$  thick) is about half the bulk density; hence, the density of the surface layer is about half the above estimate, i.e.  $\psi_{w0} = 0.62/2 = 0.31$ , provided that the distance between the “layers” does not increase near the interface. However, the latter distance most probably increases (see S1); therefore, the actual value of  $\psi_{w0}$  can be expected to fall in the range 0.31–0.63. It is noteworthy that  $\psi_{w0}$ , a characteristic of the neat surface, should be independent of the nature of the surfactant forming the monolayer.

The dependence of  $\psi_w$  on  $\psi_s$  that follows from Eq. (13), with  $\alpha_w = 6.07 \text{ \AA}^2$  and  $\alpha_s = 16.5 \text{ \AA}^2$  (as for a fatty alcohol [23]), is illustrated in Fig. 2 for three values of  $\psi_{w0}$ . It is seen that this dependence is linear at  $\psi_s \rightarrow 0$ . An expansion in series of Eq. (13) gives for this linear region the expression:

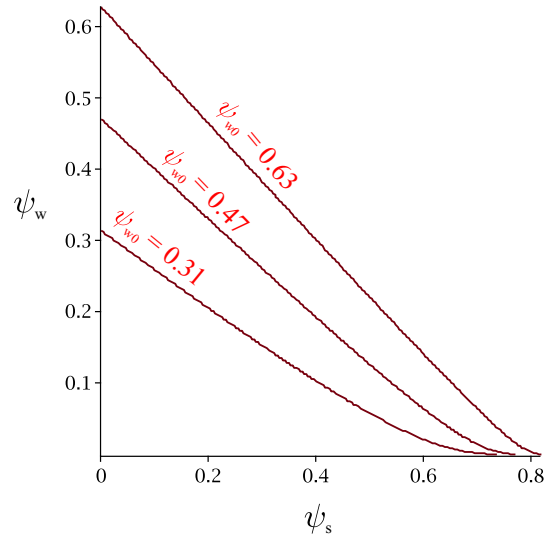


Fig. 2. Expulsion of the solvent from the adsorption monolayer: surface coverage with solvent molecules,  $\psi_w = \alpha_w \Gamma_w$ , as a function of the surfactant area fraction,  $\psi_s = \alpha_s \Gamma_s$ , according to Eq. (13) of the hard-disc mixture model ( $\alpha_w = 6.07 \text{ \AA}^2$ ,  $\alpha_s = 16.5 \text{ \AA}^2$ , and 3 different values of  $\psi_{w0}$ ; 25 °C).

$$\psi_w = \psi_{w0} - \frac{2\sqrt{r}(1 - \psi_{w0}) + (1 - \psi_{w0})^2 + r(1 + \psi_{w0})}{r(1 + \psi_{w0})} \psi_{w0} \psi_s + O(\psi_s^2). \quad (15)$$

As the density of the surfactant monolayer increases, a point is reached ( $\psi_s = 0.7-0.8$ ) where the solvent is nearly completely expelled from the surface layer. Above this point,  $\psi_w$  decreases exponentially with  $\psi_s$ ; this case (corresponding to series with respect to small  $\psi_w$ ) is analysed in S3.

By substitution of Eq. (15) into the LHP EoS (9) and expansion in series with respect to  $\psi_s$  (an approximation corresponding to a dilute 2D solution of surfactant), one obtains the following 2D osmotic virial expansion [33] of the EoS of the monolayer at fixed chemical potential of the solvent:

$$\frac{\alpha_s \pi^S}{k_B T} = \psi_s + (2 - \beta_{\text{osm}}) \psi_s^2 + \dots, \quad \text{where} \quad \beta_{\text{osm}} = \frac{2r + 4\sqrt{r} + 1 - \psi_{w0}}{2r(1 + \psi_{w0})} \psi_{w0}. \quad (16)$$

The comparison of the osmotic virial expansion (16) to the 1-component 2D gas virial expansion (6) will show that the osmotic effect on the EoS of a hard-disc monolayer is equivalent to an effective lateral attraction and leads to increased cohesiveness of the monolayer. This is illustrated in Fig. 3, where the hard-disc mixture model (the LHP EoS (9) solved numerically together with the solvent's adsorption isotherm (13) for  $\pi^S(\psi_s)$  and  $\psi_w$ ) is compared to the  $\pi^S(\psi_s)$  dependence of a 1-component hard-disc monolayer according to the HFL EoS (1), which is the limit of LHP theory in the absence of solvent. Evidently, the solvent has a significant effect on the properties of the monolayer: in the whole range of coverages, LHP predicts lower surface pressure than HFL, which corresponds to effective cohesion between the adsorbed molecules. According to Eq. (16), the value of  $\beta$  quantifying this “cohesion” is a function of the density  $\psi_{w0}$  of the surface layer at the neat surface and the surfactant/solvent hard-disc area ratio  $r$ . The osmotic attraction is larger for smaller surfactant polar head groups ( $\beta_{\text{osm}}$  increases as  $r$  decreases), as illustrated in Fig. 4.

As we shall see in the following sections, the introduction of effective osmotic attraction is useful as it allows the EoS of a cohesive surfactant monolayer in the presence of solvent to be

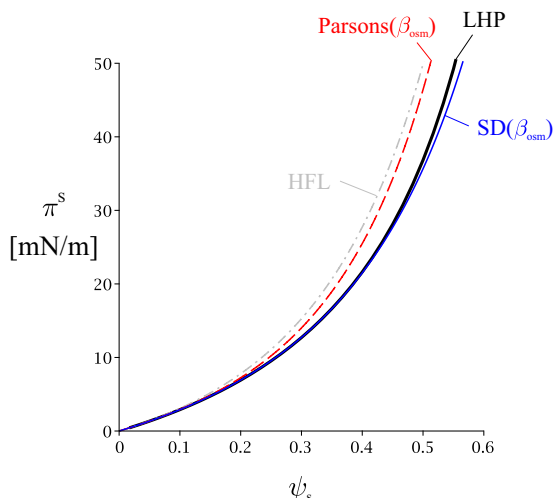


**Fig. 3.** Surface pressure  $\pi^S$  vs. surfactant coverage  $\psi_s = \alpha_s \Gamma_s$ , according to the LHP EoS (9) and the isotherm (13) for 2-component hard-disc fluid, accounting explicitly for the osmotic effect (black solid line,  $\alpha_s = 16.5 \text{ \AA}^2$ ,  $\psi_{w0} = 0.31$ , 25 °C). It is compared to the HFL model which neglects the solvent in the surface layer (grey dash-dot, Eq. (1)). The osmotic effect can be modelled as an effective depletion attraction by setting the lateral attraction parameter  $\beta$  of the EoS (2) and (3) of Parsons (red dash) and SD (blue solid) equal to the effective osmotic attraction  $\beta_{osm}$ , Eq. (16). The 1-component sticky disc model approximates well the exact 2-component LHP result. (For interpretation of the references to colour in this figure legend, the reader is referred to the web version of this article.)

simplified considerably. However, we should stress that the osmotic “attraction” does not correspond to any potential interaction between the adsorbed surfactant molecules. The solvent-induced cohesion can be understood as an entropic 2D depletion force: around each surfactant molecule, an excluded area exists which is unavailable for the solvent molecules. When two surfactant molecules approach each other, their corresponding excluded areas overlap and the total excluded area decreases (e.g., fig. 5.8 in Ref. [18]), which frees up surface for the solvent to occupy and, therefore, increases the entropy of the system. Thus, configurations of the surface with overlapping excluded areas are more probable than configurations with separated surfactant molecules, hence the depletion force. The effect is completely analogous to the 3D depletion force in mixtures of hard-disc spheres (e.g., Ref. [34,35]): the osmotic 2<sup>nd</sup> virial coefficient of the solute in such 3D mixture will be  $B_2 = 4v_s - v_s\beta_{osm}$ , where  $v_s$  is the hard-sphere volume of the solute. As an example, from the values of  $B_2$  computed for hard-sphere mixtures in table V of Pratt and Chandler [35], we find values of the 3D osmotic attraction parameter  $\beta_{osm}$  in the range 2.7–3.1 (for  $v_s/v_w = 1.1$ –1.8).

Our results can be compared with the simplistic model of Chatteraj and Birdi, who have generalized Volmer’s EoS to include the depletion effect due to the finite hard-disc area of the solvent (eq 5.15 in Ref. [18]):

$$\frac{\alpha_s \pi^S}{k_B T} = \frac{\psi_s}{1 - (1 - 1/r)\psi_s}; \quad (17)$$

similar equation has been obtained by Lucassen-Reynders and van den Tempel [36]. For small solvent molecules ( $1/r = 0$ ), this EoS reduces to Volmer’s. The virial expansion of Eq. (17) is:

$$\frac{\alpha_s \pi^S}{k_B T} = \psi_s + (1 - 1/r)\psi_s^2 + \dots \quad (18)$$

The cohesive variant of Volmer’s EoS is the 2D van der Waals EoS [37,38],  $\alpha_s \pi^S / k_B T = \psi_s / (1 - \psi_s) - \beta \psi_s^2$  (just as Parsons’ models is the cohesive variant of HFL, Eqs. (1) and (2)). The virial expansion of the van der Waals EoS reads  $\alpha_s \pi^S / k_B T = \psi_s + (1 - \beta)\psi_s^2 + \dots$ ; comparison of it with Eq. (18) shows that the osmotic attraction following

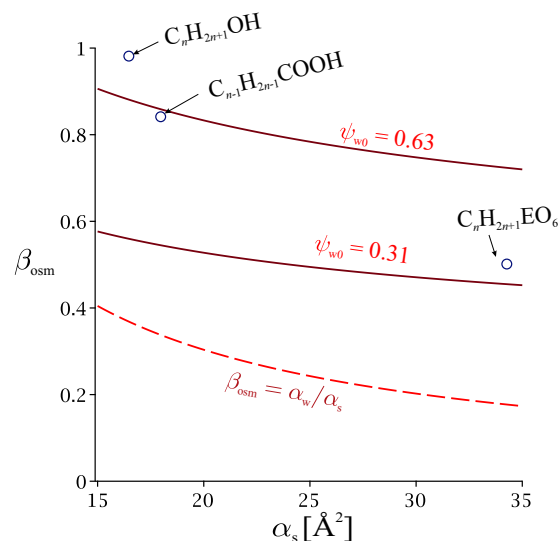


**Fig. 4.** Comparison between Eq. (16) for the osmotic attraction parameter  $\beta_{osm}$  vs. the hard-disc area of the surfactant  $\alpha_s$  (solid lines) and the osmotic lateral attraction parameters obtained from the fit of the tensiometric data for the three homologous series of surfactants in Table 1 (points). The osmotic attraction parameter  $\beta_{osm} = 1/r$  following from the model (17) of Chatteraj and Birdi is given for comparison (dashed line).

from the model of Chatteraj and Birdi corresponds to  $\beta_{osm} = 1/r$ . This result is compared to Eq. (16) for  $\beta_{osm}$  of the hard-disc mixture in Fig. 4: as seen, the qualitative behavior is similar – the osmotic cohesion is stronger for surfactants of smaller cross-section. However, the model of Chatteraj and Birdi has all problems inherent in Volmer’s model (discussed in Ref. [24]), e.g., the value of the parameter  $(1 - 1/r)\alpha_s$  in Eq. (17) has, in theory, to be smaller than  $\alpha_s$ ; instead, the fit of experimental tensiometric data with Eq. (17) always gives a value of  $(1 - 1/r)\alpha_s$  larger than the hard-disc area of the surfactant.

### 2.3. Modifying 1-component models of cohesive monolayers to account for the osmotic effect

We have shown in the previous section that the presence of solvent molecules of non-zero cross-sectional area in the monolayer results in depletion cohesion between the surfactants. It can then be expected that a model of a 1-component cohesive monolayer, such as Parsons’ or the SD EoS, can offer a good approximation to the behaviour of the hard-disc mixture, if their lateral attraction parameter  $\beta$  is set equal to  $\beta_{osm}$  from Eq. (16). A comparison between the exact LHP model of the mixture (a numerical solution to Eqs. (9) and (13)) with Parsons’ EoS (2) and the SD EoS (3) with  $\beta = \beta_{osm}$  is made in Fig. 3. It is seen that Parsons’ model deviates from the exact EoS, while the SD theory indeed approximates LHP adequately – the match is good for any physically reasonable value of  $\alpha_s$  when  $\psi_{w0} = 0.31$ ; however, if  $\psi_{w0}$  is  $>0.5$ , the differences become non-negligible. Thus, if it is ensured that the SD model has the correct 2<sup>nd</sup> virial coefficient, including the osmotic effect, this 1-component model becomes nearly equivalent to the more advanced hard-disc mixture theory of LHP.

This finding allows us to make an approximate but straightforward extension of the hard-disc mixture model to attractive molecules. A monolayer made of surfactant molecules interacting between each other with an attractive potential  $u_{attr}$ , and containing solvent molecules penetrating the monolayer as sketched in Fig. 1, can be expected to follow the 1-component SD model (3)–(5) with lateral attraction parameter given by the sum

$$\beta = \beta_{attr} + \beta_{osm}, \quad (19)$$

where  $\beta_{\text{attr}}$  is related to  $u_{\text{attr}}$  via Eq. (7), and  $\beta_{\text{osm}}$  is the contribution (16) from the solvent.

This simple rule explains the apparent success of the SD model in predicting the behaviour of monolayers adsorbed at liquid interfaces found in Ref. [24], despite the fact that the solvent molecules have been neglected. A more detailed analysis would show that the good coincidence with the experimental data is, in fact, due to a compensation of effects. The formula (7) and (8) for the van der Waals contribution to  $\beta$  has been used in Ref. [24] under the assumption that all  $\text{CH}_2$  groups contribute equally to the lateral attraction ( $\beta = \beta_{\text{vdW},n}$ ). However, there is enough evidence that one methylene group remains immersed in the aqueous phase, probably due to the polarization effect of the polar head group on the adjacent  $\text{CH}_2$ . The immersed  $\text{CH}_2$  should not contribute significantly to  $\beta$ , as the van der Waals interaction between  $\text{CH}_2$  groups through water is weak [28]. This immersion effect is especially clear in two cases: (i) with fatty acids, where only  $n - 1$  carbon atoms should contribute to  $\beta$  as the first carbon is in a carbonyl ( $> \text{C}=\text{O}$ ) group (whereas in Ref. [24] it was assumed that all  $n$  carbons contribute); and (ii) with alkyldimethylphosphineoxides, where the two  $\text{CH}_3$  groups attached to the polar head group contribute neither to the adsorption constant  $K_a$  nor to the attraction parameter  $\beta$  of these surfactants, i.e. these methyl groups behave as a part of the polar head [24]. A similar immersion effect has been noticed with micelles (Chap. 3 and Eq. 6–4 of Tanford [39]; see also Ref. [40]). Thus, instead of our previous assumption  $\beta = \beta_{\text{vdW},n}$ , a more realistic model of  $\beta$  would account explicitly for both the solvent molecules in the monolayer and the immersion of one  $\text{CH}_2$  group as:

$$\beta = \beta_{\text{vdW},n-1} + \beta_{\text{osm}}. \quad (20)$$

A hydrophobic chain shorter by one methylene group corresponds to a smaller van der Waals attraction, which compensates for the neglected osmotic attraction (i.e.  $\beta_{\text{vdW},n-1} + \beta_{\text{osm}} \approx \beta_{\text{vdW},n}$ , see S2) and leads ultimately to the adequate comparison with the experiment observed in Ref. [24]. In the following section, we will take an explicit account for both the osmotic and the immersion effects when comparing with tensiometric data, to show that the compensation is often, but not always, efficient.

Before turning to the experimental data, let us summarize the limitations of the sticky disc model:

- (i) Water is an associated liquid. The hard-sphere models are quite successful in predicting numerous properties of aqueous solutions [41], yet, a hard-disc model can only offer a first approximation to the aqueous surface's structure. Corrections for the association and the dipole-dipole interactions are an important next step towards a thorough theory (the SD model involves only surfactant-surfactant interaction), and would make the difference between the 2D depletion force we analyse and a 2D hydrophobic effect. Qualitatively, by analogy with the respective 3D theory (table 5 in Ref. [35]), we can hypothesize that, if the water H-bonded structure is taken into account,  $\beta_{\text{osm}}$  will increase in comparison with the hard-disc formula (16), especially at large  $\alpha_s$ .
- (ii) The monolayer assumption is rather crude, especially when the polar head group of the surfactant is large.
- (iii) The SD model corrected for the osmotic effect does not coincide completely with the 2-component LHP. The assumption (20) for additivity of the van der Waals attraction and the osmotic cohesion is not necessary accurate.
- (iv) The model of the lateral attraction is also crude, as it neglects, e.g., the direct interaction between the polar head groups. The role of the normal dipole moment of the monolayer is also neglected [42].

### 3. Comparison with experimental data

#### 3.1. Surface tension and surfactant adsorption

The most common experimental source of information for the state of soluble monolayers is tensiometry ( $\sigma$  vs.  $C_s$  data). In order to determine the values of the osmotic attraction parameter  $\beta_{\text{osm}}$ , we will use surface tension data at W/A for three homologous series of surfactants having head-groups of different hard-disc areas: alkanols, non-dissociated carboxylic acids, and hexaethyleneglycol alkyl ethers (alkanol hexaethoxylates,  $\text{C}_n\text{H}_{2n+1}(\text{OC}_2\text{H}_4)_6\text{OH}$  or  $\text{C}_n\text{H}_{2n+1}\text{EO}_6$ ). A direct fit of tensiometric data for a single surfactant with any adsorption model suffers from large uncertainty of the involved adsorption parameters, especially  $\alpha_s$  and  $\beta$  [24]. In addition, the disagreement between the available data for the same surfactant from different authors often leads to misleading results (an example is given below). To minimize these errors, we will use the theoretically expected values for all adsorption parameters which can be determined independently, drawing on the work of Ivanov et al. [20,22–24,43], as follows.

- (i) We use crystallographic or monolayer collapse data (cf. S1) to determine the hard-disc area  $\alpha_s$  of the surfactant independently, instead of fitting with it. The alcohol group is of cross-sectional area smaller than that of the hydrocarbon chain, so we used crystallographic data for solid alkanes [44,45] together with areas of collapse of insoluble monolayers of alcohols [46,47]: these data yield an average area per molecule in a close-packed structure of  $\alpha_{\perp} = 18.2 \pm 0.4 \text{ \AA}^2$ . This value has to be corrected by a packing factor: for hexagonal packing,  $\alpha_{\perp}$  must be divided by 1.10 (the ratio between the area of a hexagon and the inscribed circle) to obtain the actual area  $\alpha_s = 16.5 \pm 0.4 \text{ \AA}^2$  of the hard disc. For acids, we used data for the collapse area of several insoluble long-chained homologues [17,48–50]. The average value of these data is  $\alpha_{\perp} = 19.8 \pm 0.8 \text{ \AA}^2$ , which is close to the crystallographic area  $20.5 \text{ \AA}^2$  quoted by Langmuir [48], and to the average  $\alpha_{\perp} = 20.05 \text{ \AA}^2$  following from the crystallographic data of Bond [51] (calculated as explained in S1). The relatively large uncertainty ( $\pm 0.8 \text{ \AA}^2$ ) is probably related to the slightly different  $\alpha_{\perp}$  of the acids with even or odd number of carbons (from Bond's data,  $\alpha_{\perp} = 19.0$  or  $20.4 \text{ \AA}^2$ , respectively [51]). Using the correction factor for close packing 1.10, we find for the hard-disc area  $\alpha_s = 18.0 \pm 0.8 \text{ \AA}^2$  for acids. The collapse area of the ethoxylate monolayer can be estimated from the surface pressure isotherm of Lange and Jeschke [52] for hexaethoxylate spread on concentrated  $\text{NaNO}_3$ , which ends at  $\alpha_{\perp} = 37.8 \text{ \AA}^2$ , where presumably the collapse occurred; with the correction factor 1.1 for hexagonal packing, this gives  $\alpha_s = 34.2 \text{ \AA}^2$ . This value is in good agreement with  $36.3 \text{ \AA}^2$  obtained by Nikas et al. [19] by a Monte Carlo-rotational isomeric state simulation of a hexaethoxylate chain attached at one end to an ideal solid. However, the collapse area has, in principle, a small but non-negligible dependence on the salt concentration (as evident, e.g., from fig. 5 in Ref. [47]), which puts a question mark over the collapse value above, and the theoretical value of Nikas et al. is based on a somewhat arbitrary criterion for identification of the average length of the  $\text{EO}_6$  group. Therefore, instead of using  $\alpha_s = 34.2$  or  $36.3 \text{ \AA}^2$ , we left  $\alpha_s$  of  $\text{C}_n\text{H}_{2n+1}\text{EO}_6$  as an adjustable parameter to be determined from the experimental data. For all three homologous series, the areas  $\alpha_{\perp}$  and  $\alpha_s$  are, to a good approximation, independent of  $n$ .
- (ii) For the dependence of the adsorption constant  $K_a$  on  $n$ , we utilize Traube's rule:

$$\ln K_a = \ln K_{a0} + n\Delta\mu_{\text{CH}_2}/k_B T. \quad (21)$$

For all surfactants, we used the known value for the free energy of transfer of a  $\text{CH}_2$  group from air to water,  $\Delta\mu_{\text{CH}_2}/k_B T = 1.04 \pm 0.06$  [43], an average obtained from adsorption data for numerous ionic and non-ionic surfactants. The intercept  $\ln K_{a0}$  in Eq. (21) is a characteristic of the whole homologous series. Since it is a very sensitive parameter, it will be left as a fitting parameter. To check how reasonable are the obtained values of  $\ln K_{a0}$ , we will use the recent theory of Ivanov et al., which, to a good approximation, can be formulated as:

$$\ln K_{a0} = \ln \delta_a + \alpha_{\perp} \sigma_0 / k_B T; \quad (22)$$

this is eq. 27 in Ref. [24], with contribution of the polar head  $\Delta\mu_{\text{head}} = -\Delta\mu_{\text{CH}_2}$  due to the immersion of the methylene group adjacent to the head group, and  $\Delta\mu_{\text{CH}_3} \approx 2\Delta\mu_{\text{CH}_2}$  for the energy of transfer of a  $\text{CH}_3$  group from air to water. Here,  $\delta_a = l_{\text{CH}_2} k_B T / 2\Delta\mu_{\text{CH}_2}$  is Ivanov's adsorption length; its value is very different from the empirical assumption that  $\delta_a = n l_{\text{CH}_2}$  which is very common in the literature [53,54]. The term  $\alpha_{\perp} \sigma_0$  stands for the free energy of the portion of neat surface that disappears upon adsorption of a molecule, and has occurred in several mechanistic models of  $K_a$  (e.g., [55]). The term  $\alpha_{\perp} \sigma_0$  has been shown to have a large contribution to the heat of adsorption [43]; it also explains the effect of the nature of the oil phase on the adsorption constant at various water/oil interfaces [23]. In this work, we will test another prediction: according to Eq. (22), the energy  $\alpha_{\perp} \sigma_0$  is the sole reason for the different adsorption constants of the three surfactant series at the same value of  $n$ .

- (iii) Finally, for the lateral attraction parameter, we use Eqs. (7), (8) and (20), with  $\beta_{\text{vdW},n-1}$  corresponding to attractive potential  $u_{\text{attr}}$  involving only those  $n-1$   $\text{CH}_2$  groups that are not immersed in the aqueous phase. Written explicitly in a form convenient for numerical integration, Eq. (20) reads:

$$\beta = \beta_{\text{osm}} + \frac{\pi}{\tilde{\alpha}_s} \int_{2\sqrt{\tilde{\alpha}_s/\pi}}^{\infty} \left[ \exp\left(\frac{\tilde{\rho}^2 + 3\arctan(\tilde{\rho})}{4\tilde{\rho}^5}\right) - 1 \right] \tilde{\rho} d\tilde{\rho}, \quad \text{where} \quad (23)$$

$$\tilde{T} = (n-1)^4 l_{\text{CH}_2}^6 k_B T / L_{\text{CH}_2}, \quad \tilde{\alpha}_s = \alpha_s / (n-1)^2 l_{\text{CH}_2}^2.$$

We will leave the osmotic contribution  $\beta_{\text{osm}}$  as a free fitting parameter, assuming that it is independent of  $n$ , as predicted by the hard-disc mixture formula (16).

We are aware of only two statistical mechanical model of  $\beta$  which could be compared to Eqs. (8) and (23). Nikas et al. [19] used a similar formula, but with three differences: (i) they used  $u_{\text{attr}}$  expanded into series for large  $n$  ( $u_{\text{attr}} = -3\pi n L_{\text{CH}_2} / 8 l_{\text{CH}_2} \rho^5$  instead of Eq. (8)), an approximation that fails for surfactants of  $ca. n < 8$ ; (ii) they used a value of the London constant twice as large as ours; (iii) they neglected the osmotic contribution  $\beta_{\text{osm}}$ . The last two approximations compensate to a certain extent for the surfactants studied in Ref. [19]. The other model – the semi-empirical linear formula of Smith [17] – has been discussed previously [24].

Let us note that we have previously shown that the hard-disc area  $\alpha_s$  can be substituted with what follows from collapse and crystallographic data only if an appropriate delocalized model is used – the areas of the molecule following from the popular models of Volmer, van der Waals, Langmuir, Frumkin and others are always no more than empirical parameters, much higher than the crystallographic area, and are not transferable to, e.g., water/oil interface. In addition, the formulae (7) and (8) for  $\beta$  are compatible with the sticky disc model (3), but – especially with strongly cohesive surfactants – not with cohesive models based on the correction  $\beta\psi_s^2$  in the EoS (such as Parsons', van der Waals', Frumkin's, or the one of Nikas et al.) [24].

To recapitulate, instead of using 3 adjustable parameters ( $K_a$ ,  $\alpha_s$  and  $\beta$ ) for each surfactant in a homologous series (or a total of 21 parameters for 7 alcohols or acids), the molecular thermodynamic model (i-iii) allows us to use two or three parameters ( $K_{a0}$ ,  $\beta_{\text{osm}}$ , and for the  $\text{C}_n\text{H}_{2n+1}\text{EO}_6$  – also  $\alpha_s$ ) for a whole homologous series. Even for these three parameters, we have reliable independent estimates that would allow us to judge how reasonable the fitted values are.

The tensiometric dataset used for the optimization for a given homologous series is composed of 3 columns – the dependent experimental variable  $\pi^S$  measured as a function of the surfactant concentration  $C_s$  and the chain length  $n$ . The respective merit function we use for the optimization has the form:

$$\text{dev}^2(K_{a0}, \beta_{\text{osm}}) = \frac{\sum [\pi_{n,i}^S - \pi_{\text{th}}^S(C_i, n; K_{a0}, \beta_{\text{osm}})]^2}{N-2}, \quad (24)$$

where  $\pi_{n,i}^S$  is the  $i^{\text{th}}$  experimental surface pressure value for the  $n^{\text{th}}$  homologue,  $\pi_{\text{th}}^S$  is the theoretical value following from the SD model (3)–(5) at the  $i^{\text{th}}$  experimental surfactant concentration  $C_i$ , with  $K_a$  given by Eq. (21) and  $\beta$  given by Eq. (23). The sum is over all homologues and data points, a total of  $N$  points. For the hexaethyleneglycol alkyl ethers, the hard-disc area  $\alpha_s$  of the surfactant was also left as a free fitting parameter, while for alcohols and acids we used the areas 16.5 and 18.0  $\text{\AA}^2$  that follow from crystallographic and collapse data.

For alcohols, we analysed W/A surface tension data for homologues from propanol to decanol from a number of authors [9,12,56–64], a total of  $N = 203$  data points; these measurements were done at an average temperature of  $21 \pm 1$  °C. The data for propanol were corrected for non-ideality as explained in Ref. [24]. For the carboxylic acids from  $\text{C}_2\text{H}_5\text{COOH}$  to  $\text{C}_9\text{H}_{19}\text{COOH}$ , we assembled tensiometric data at low pH and average temperature of  $21 \pm 1$  °C from Refs. [10,62,65–68],  $N = 163$  points. The data for hexaethyleneglycol monododecyl and monotetradecyl ethers (dodecanol- and tetradecanol hexaethoxylate,  $\text{C}_n\text{H}_{2n+1}\text{EO}_6$ ) are from Refs. [9,11,12,69], at 25 °C, 46 points. An Excel spreadsheet with the data is provided as a supplement S6.

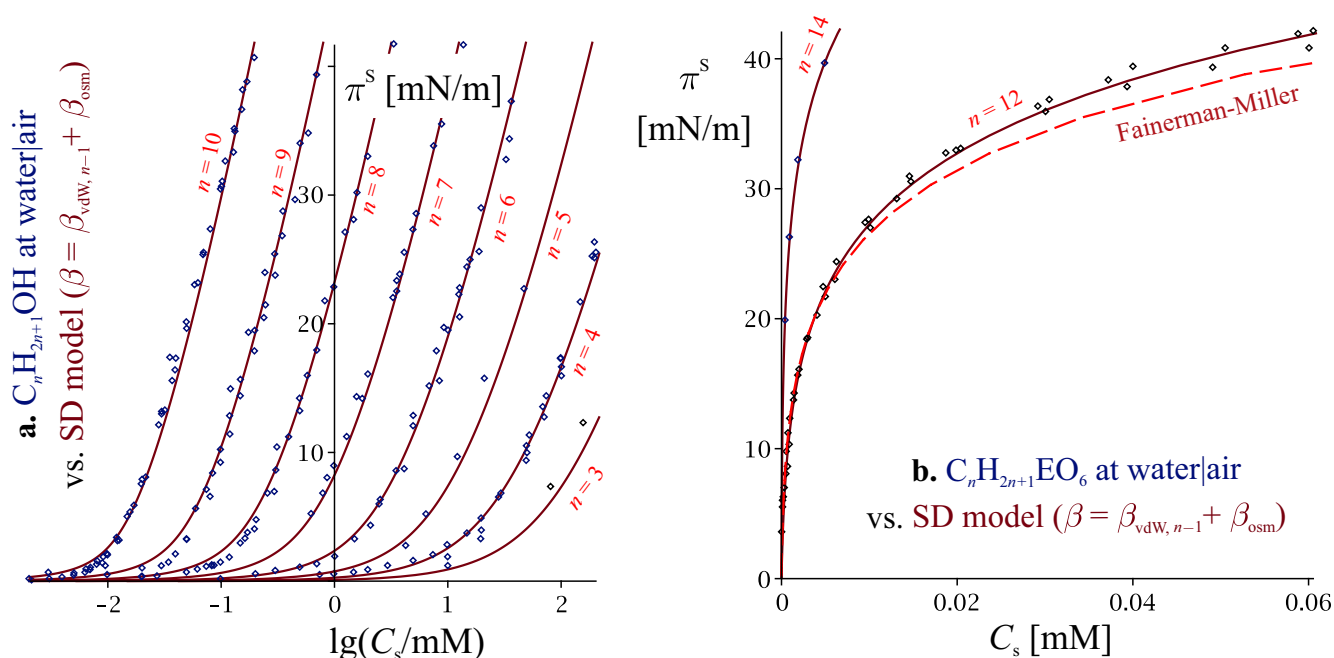
The results from the minimization of the dispersion (24) are summarized in Table 1 for the three series. There, they are compared with the previous variant of the SD model used in Ref. [24], which neglects the osmotic attraction and the  $\text{CH}_2$  immersion (i.e.  $\beta = \beta_{\text{vdW},n}$ ). The improvement of the standard deviation when the osmotic and the immersion effects are explicitly accounted for is quite significant for the *alcohols* (the standard deviation drops from 1.44 to 0.97 mN/m, Table 1). The predictions of the corrected SD model are compared with the data in Fig. 5a, and the two variants of the SD model are compared in S2. On the contrary, for *acids*, the results of the two variants of SD are practically equivalent in terms of standard deviation; the comparison with the data is given in S2, but the compensation between the osmotic/depletion and the immersion effect for acids is nearly complete, so the theoretical lines are close to those obtained previously in Ref. [24]. Fig. 5b illustrates the results for  $\text{C}_n\text{H}_{2n+1}\text{EO}_6$ .

As an independent test of our model, we compared available neutron reflection data for the adsorption of butanol, hexanol [70], and  $\text{C}_{12}\text{H}_{25}\text{EO}_6$  [71] with the adsorption isotherm (4) and (5) of the SD model, with  $K_{a0}$  and  $\beta_{\text{osm}}$  as obtained from the fit of the tensiometric data. The comparison with the data for butanol is excellent, as shown in Fig. 6. The adsorption data for hexanol and  $\text{C}_{12}\text{H}_{25}\text{EO}_6$  both show similar negative deviations from the theoretical line, discussed in S2.

Let us now consider the values we obtained for the adsorption parameters. The fit gives  $\ln(K_{a0}/\text{m}) = -20.2$ ,  $-20.1$ , and  $-16.9$  for the alkanols, the acids and the hexaethoxylates, respectively (Table 1). On the other hand, the theoretical values computed

**Table 1**Adsorption parameters of 3 homologous series of surfactants on water, obtained by minimization of Eq. (24) using the sticky disc model with  $\beta$  given by Eq. (20).

Homologous series	$\ln(K_{a0}/m)^c$	$\alpha_s$ [ $\text{\AA}^2$ ]	$\beta = \beta_{vdW} + \beta_{osm}^e$	$dev$ [mN/m]
$C_nH_{2n+1}OH^a$	-20.4 -20.2	16.5 <sup>d</sup>	$\beta_{osm} = 0, \beta_{vdW,n}$ $\beta_{osm} = 0.98, \beta_{vdW,n-1}$	1.44 0.97
$C_{n-1}H_{2n-1}COOH^a$	-20.2 -20.1	18 <sup>d</sup>	$\beta_{osm} = 0, \beta_{vdW,n}$ $\beta_{osm} = 0.84, \beta_{vdW,n-1}$	0.93 0.90
$C_nH_{2n+1}EO_6^b$	-16.82 -16.89	33.3 34.3	$\beta_{osm} = 0, \beta_{vdW,n}$ $\beta_{osm} = 0.50, \beta_{vdW,n-1}$	0.67 0.655

<sup>a</sup> The data are for  $n = 3 \div 10$ , average  $T = 21$  °C.<sup>b</sup> Data for  $n = 12$  and  $14$ ,  $T = 25$  °C.<sup>c</sup> The transfer energy in the expression (21) for the adsorption constant  $K_a$  is fixed to  $\Delta\mu_{CH_2} = 1.04 \times k_B T$  [43].<sup>d</sup> Value of the hard-disc area calculated from crystallographic and collapse data of alcohols and acids, see the text.<sup>e</sup> Fixed to the value predicted by Eq. (23), with  $n$  or  $n - 1$   $CH_2$  groups contributing to  $\beta_{vdW}$ , with or without  $\beta_{osm}$ .

**Fig. 5.** (a) Surface pressure  $\pi^S$  vs. decimal logarithm of the surfactant concentration  $C_s$  of alcohols at W|A. Lines stand for the SD model with attraction parameter  $\beta = \beta_{osm} + \beta_{vdW,n-1}$  (corrected for the solvent effect and for one immersed methylene group, Eq. (23)). Two adjustable parameters for the whole homologous series were determined:  $\ln(K_{a0}/m) = -20.2$  and  $\beta_{osm} = 0.98$ . (b) Surface pressure  $\pi^S$  vs. surfactant concentration  $C_s$  of  $C_nH_{2n+1}EO_6$ . Lines are the SD model with  $\ln(K_{a0}/m) = -16.9$ ,  $\alpha_s = 34.3 \text{ \AA}^2$ , and  $\beta_{osm} = 0.5$ . The reorientation model of Fainerman and Miller [9] is plotted for comparison.

through Ivanov's model are  $\ln(K_{a0}/m) = -20.3$ ,  $-20.0$ , and  $-16.9$ . The agreement is remarkable, and shows that the dependence of the adsorption constant on the nature of the polar head group of the surfactant is indeed due to the term  $\alpha_s \sigma_0$  in Eq. (22). Therefore, the well-known tendency of  $K_a$  to increase with each ethyleneglycol group added (e.g., table 3.13 in Ref. [9]) seems to be related to the respective increase of the hard-disc area of the  $EO_m$  group.

The hard-disc area of the  $C_nH_{2n+1}EO_6$  found from the fit is  $34.3 \text{ \AA}^2$  (Table 1). This is practically equivalent to the value  $\alpha_s = 34.2 \text{ \AA}^2$  following from the collapse area of Lange and Jeschke [52] discussed above.

Let us now discuss the two effects – from the solvent in the monolayer and from the immersion – on the values of the lateral attraction parameter. The values of  $\beta$  that follow from Eq. (23) for all studied surfactants are summarized in Table 3 in S2, where they are compared to the approximation  $\beta = \beta_{vdW,n}$  neglecting the two effects. Despite the compensation of effects, the difference between  $\beta_{osm} + \beta_{vdW,n-1}$  and  $\beta_{vdW,n}$  is not small, especially for alcohols. With regard to the osmotic parameter, the fitted value in Table 1 found for alcohols ( $\beta_{osm} = 0.98$ ) corresponds, according to Eq. (16), to  $\psi_{w0} = 0.77$ ; the value for the acids ( $\beta_{osm} = 0.84$ ) corresponds to  $\psi_{w0} = 0.61$ , and  $\beta_{osm} = 0.50$  for the ethyleneglycol ethers

corresponds to  $\psi_{w0} = 0.36$ . Clearly,  $\beta_{osm}$  decreases as  $\alpha_s$  increases, in qualitative agreement with Eq. (16), as illustrated in Fig. 4. However, while the qualitative trend with  $\alpha_s$  and the order of magnitude of  $\beta_{osm}$  are very reasonable, quantitatively, there is a discrepancy. This is not surprising, in view of the limitations of the model, (i-iv) in Sec. 2.3. In addition, the uncertainty of the  $\beta_{osm}$  values we obtained is not small. Our adsorption model is much more sensitive to  $\alpha_s$  and  $\Delta\mu_{CH_2}$  than to  $\beta_{osm}$  – a small change in the values of  $\alpha_s$  and  $\Delta\mu_{CH_2}$  has an effect on the adsorption behaviour comparable with the osmotic effect we consider. Yet, we use for them independent estimates that are not too accurate ( $\Delta\mu_{CH_2}/k_B T = 1.04 \pm 0.06$ ;  $\alpha_s = 16.5 \pm 0.4 \text{ \AA}^2$  for alcohols and  $18.0 \pm 0.8 \text{ \AA}^2$  for acids). If we vary these parameters within their uncertainty limits, the results for  $\beta_{osm}$  will change significantly.

Extensive comparison of the SD theory with other models has been given previously [24]; one model we did not consider there (as only surfactants of relatively simple head groups were analysed) was the reorientation model of Fainerman and Miller [9]. This is a typical localized EoS based on Langmuir's. According to Fainerman and Miller, surfactants such as alkanol polyethoxylates have two stable conformations at the surface, corresponding to



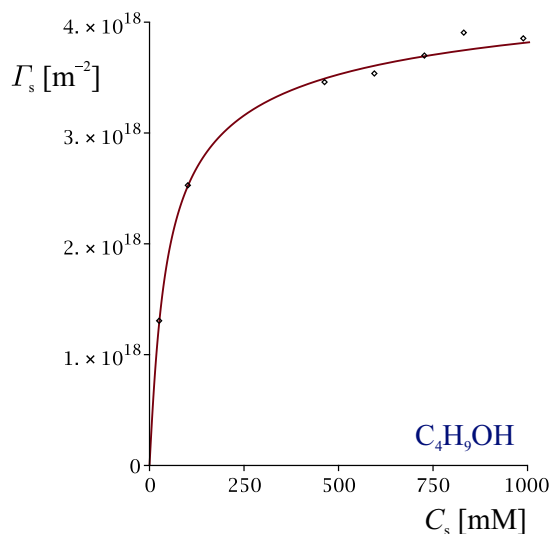


**Fig. 6.** Adsorption of butanol at W|A vs. surfactant concentration  $C_s$ . Points: neutron reflection data from Ref. [70]. Line: the SD adsorption isotherm (4) and (5), with the hard-disc area  $\alpha_s = 16.5 \text{ \AA}^2$ , attraction parameter  $\beta$  calculated from Eq. (23), and adsorption constant  $K_s$  from Eq. (21), with  $K_{s0}$  and  $\beta_{osm}$  from Table 1.

two populations of adsorbed molecules, characterized by two respective area parameters and two adsorption energies. Using the parameters for  $C_{12}H_{25}EO_6$  from table 3.13 of Ref. [9] in eqs. 3.3–3.9 there, we calculated the surface pressure and the adsorption of this surfactant as functions of the concentration as predicted by the reorientation model. The result for the surface pressure is the dashed line in Fig. 5b, and it stands below the experimental data. This is entirely due to the fact that Fainerman and Miller used different sources (including some data at a different temperature), which do not agree well with each other; actually, it is not a problem to fit with a 4-parametric model the tensiometric data in Fig. 5b to within its experimental uncertainty. Moreover, in S2, it is shown that the reorientation model compares better with the adsorption data directly obtained from neutron scattering than the SD model does. This only shows that when two models describe a dataset well, a small difference in the respective deviations is not a useful criterion to distinguish between them. What matters is how sensible are the parameter values. The area of the contracted state of the monolayer obtained in Ref. [9] is  $49.3 \text{ \AA}^2$ ; this is much bigger than the collapse area  $\alpha_{\perp} = 37.8 \text{ \AA}^2$  obtained in Ref. [52], i.e. a situation that is difficult to explain occurs, where the monolayer can be experimentally compressed to values smaller than the theoretically possible limit predicted by the reorientation model. This paradox occurs every time when localized theories (Langmuir's, Frumkin's etc.) are applied to data for liquid interfaces, but disappears when the appropriate delocalized models are utilized [24]. In addition, the model of Fainerman and Miller ignores completely the lateral attraction between the hydrocarbon chains of  $C_{12}H_{25}EO_6$ , while the direct computation via Eqs. (7) and (8) shows a non-negligible value of  $\beta_{vdW,n-1} = 0.93$ .

Let us finally remark that the reorientation effect is relatively straightforward to implemented in a delocalized hard-disc mixture model – this has been already done by Fraser et al. [31], in the absence of solvent and attraction.

### 3.2. Solvent expulsion from the monolayer and neutron reflectivity

A unique feature of our model is that the knowledge of the value of  $\beta_{osm}$  allows us to estimate the decrease of the amount of solvent in the surface layer upon adsorption of surfactant, through the isotherm of the solvent. For example, for  $C_nH_{2n+1}EO_6$ , from the

fitted values  $\beta_{osm} = 0.50$  and  $\alpha_s = 34.3 \text{ \AA}^2$ , we find  $\psi_{w0} = 0.36$  through Eq. (16). Using this  $\psi_{w0}$  in the adsorption isotherm of the solvent of the hard-disc mixture model, together with the SD adsorption isotherm for the surfactant, we can compute the surface fractions of water and surfactant as functions of the surfactant bulk concentration  $C_s$ . This is done in Fig. 7. The results for the alcohols are similarly dealt with in S2. Due to the limitations of the model (Sec. 2.3), the result for the water content  $\psi_w$  and the total coverage  $\psi_w + \psi_s$  is probably a crude approximation ( $\psi_s$ , on the other hand, must be accurate since any reasonable interpolation of the tensiometric data will produce the correct surfactant adsorption). Nevertheless, the trends observed are reasonable:

- (i) the solvent surface fraction drops and approaches zero as more surfactant adsorbs;
- (ii) the total coverage (total density of the monolayer) increases with the increase of  $\psi_s$ .

Note that the hard-disc mixture model predicts that the monolayer is of total coverage significantly lower than 1, and has a large compressibility. In contrast, both approaches that Frumkin cited in defence of the Langmuir model [1,6] assume that the monolayer is incompressible and  $\psi_w + \psi_s = 1$ ; the same is valid for the EoS of Chatteraj and Birdi [18].

The predicted expulsion of water from the monolayer has a well-defined effect on the location of the Gibbs equimolecular surface – according to Eq. (32) in S1, the shift  $\Delta z^S$  of this surface with respect to the centre of the surface layer is given by

$$\Delta z^S = \frac{V_w}{\alpha_w} \left( \frac{1}{2} - \psi_w \right). \quad (25)$$

The shift  $\Delta z^S$  leads to larger separation between the surfactant centre of mass and water's equimolecular surface as  $\psi_w$  decreases (i.e. as more surfactant adsorbs), as schematically shown in Fig. 8. A direct measure of this separation is the quantity  $\delta_{sw}$  calculated by Li et al. from their neutron reflection data [70], which is defined as the distance between the centres of the assumed distributions of the scattering densities of the water and the alcohol.

The value of  $\delta_{sw}$  has been found to increase with the adsorption of surfactant (Table 2). This tendency has been interpreted by Li

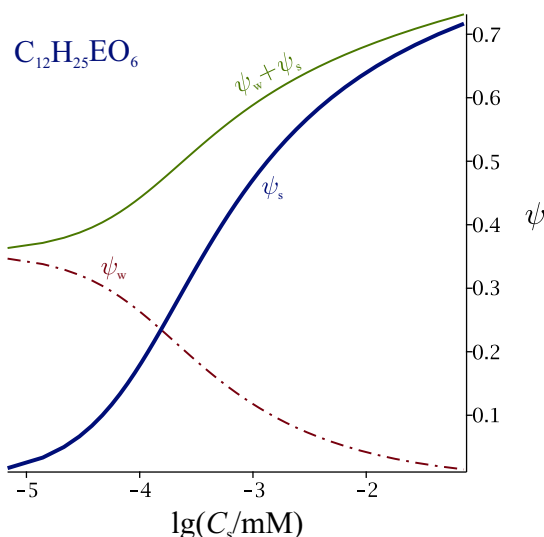


**Fig. 7.** Surface coverage with solvent ( $\psi_w = \alpha_w \Gamma_w$ ), surfactant ( $\psi_s = \alpha_s \Gamma_s$ ), and total ( $\psi_w + \psi_s$ ) vs. the logarithm of surfactant concentration in the bulk phase for hexaethylglycol monododecyl ether. Eq. (13) is used to compute  $\psi_w$  and Eqs (4) and (5) are used to compute  $C_s$  for a set of values of  $\psi_s$  to plot these curves.

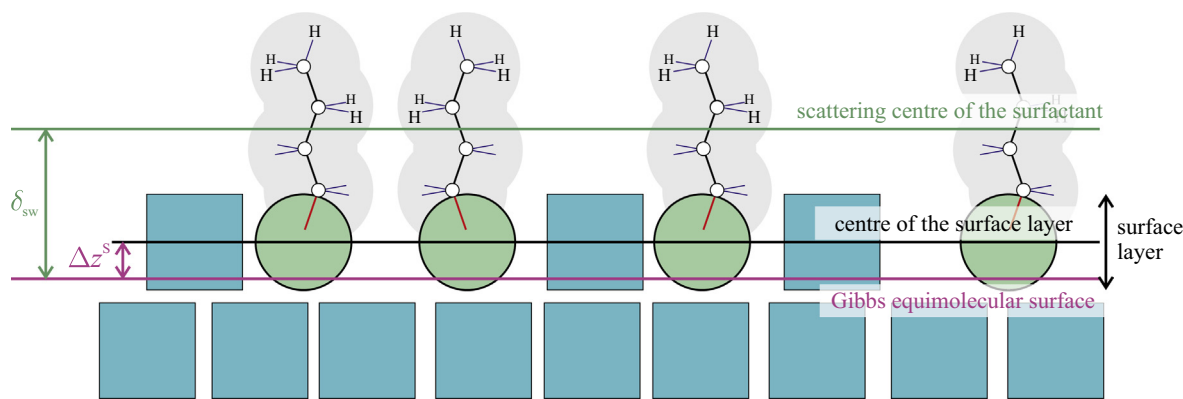


**Fig. 8.** Schematic definition of the shift  $\Delta z^S$  of the equimolecular surface of water, and the separation  $\delta_{sw}$  between the equimolecular surface and the “scattering centre” of the alcohols.

**Table 2**

Relationship between the surface fraction of solvent and the separation between the surfactant centre of mass and the Gibbs equimolecular surface of butanol and hexanol.

<i>butanol</i>					
$1/\Gamma_s$ [ $\text{\AA}^2$ ] <sup>a</sup>	75	39	28	25	
$\psi_s$ <sup>b</sup>	0.22	0.42	0.59	0.66	
$\psi_w$ <sup>c</sup>	0.57	0.39	0.24	0.18	
$\Delta z^S$ [ $\text{\AA}$ ] <sup>d</sup>	−0.36	0.55	1.28	1.59	
$\delta_{sw}$ [ $\text{\AA}$ ] <sup>a</sup>	$2 \pm 1$	$2 \pm 0.5$	$3 \pm 0.5$	$4 \pm 0.5$	
$\delta_{sw} - \Delta z^S$ [ $\text{\AA}$ ]	2.4	1.5	1.7	2.4	
average $\delta_{sw} - \Delta z^S = 2.0 \pm 0.5 \text{ \AA}$					
<i>hexanol</i>					
$1/\Gamma_s$ [ $\text{\AA}^2$ ] <sup>a</sup>	130	62	50	36	28
$\psi_s$ <sup>b</sup>	0.13	0.27	0.33	0.46	0.59
$\psi_w$ <sup>c</sup>	0.66	0.53	0.47	0.36	0.24
$\Delta z^S$ [ $\text{\AA}$ ] <sup>d</sup>	−0.77	−0.15	0.13	0.70	1.28
$\delta_{sw}$ [ $\text{\AA}$ ] <sup>a</sup>	$2 \pm 1$	$2.5 \pm 1$	$3 \pm 0.5$	$3.5 \pm 0.5$	$3.5 \pm 0.5$
$\delta_{sw} - \Delta z^S$ [ $\text{\AA}$ ]	2.8	2.65	2.9	2.8	2.2
average $\delta_{sw} - \Delta z^S = 2.7 \pm 0.25 \text{ \AA}$					

<sup>a</sup> Neutron reflectivity data from Ref. [70].

<sup>b</sup> Surface fraction of surfactant calculated as  $\psi_s = \alpha_s \Gamma_s$  using  $\alpha_s = 16.5 \text{ \AA}^2$ .

<sup>c</sup> Surface fraction of the solvent calculated as the solution to the solvent’s isotherm (13) with  $r = \alpha_s/\alpha_w = 2.72$  and  $\psi_{w0} = 0.77$  for alcohols.

<sup>d</sup> Shift of the Gibbs equimolecular surface with respect to the centre of the monolayer according to Eq. (25), cf. Fig. 8.

et al. as thickening of the surfactant layer due to a change in the tilt of the adsorbed hydrocarbon chains. However, the values calculated in Table 2 for  $\psi_w$  from the solvent’s isotherm (13), and for the respective shift  $\Delta z^S$  through Eq. (25), draw a very different picture – namely, that the increase of  $\delta_{sw}$  with  $\Gamma_s$  is most of all due to the solvent being expelled from the surface layer. Subtraction of the squeezing-out effect from the total separation gives the quantity  $\delta_{sw} - \Delta z^S$ , which should depend on the tilt of the surfactant only – as seen in Table 2, within the uncertainty of  $\delta_{sw}$  ( $>0.5 \text{ \AA}$ ),  $\delta_{sw} - \Delta z^S$  is constant, suggesting that the surfactant tilt changes little in the studied range of areas per molecule, both for butanol and hexanol.

The absolute values of  $\delta_{sw} - \Delta z^S$  that follow from the schematic in Fig. 8 are  $3/2l_{\text{CH}_2} + l_{\text{CO}} = 3.1$  and  $5/2l_{\text{CH}_2} + l_{\text{CO}} = 4.3 \text{ \AA}$  for butanol and hexanol standing upright (where  $l_{\text{CO}} = 1.17 \text{ \AA}$  is the length of the CO bond along the axis of the hydrocarbon chain). This is by 1.1 and 1.6  $\text{\AA}$  larger than the respective experimental values in Table 2. Two limiting explanations are possible for this difference. The first is that it is due to a density-independent average tilt of the hydrocarbon chain of about  $50^\circ$  off the normal. The second is that one  $\text{CH}_2$  group, of length  $1.26 \text{ \AA}$ , remains immersed in water (thus, three experimental parameters –  $K_a$ ,  $\beta$  and  $\delta_{sw}$  – would be in agreement with the assumption for one immersed  $\text{CH}_2$  group). Of course, any combination of these two effects is also a possible explanation.

Li et al. [70] determined two other geometric characteristics of the structure of the alcohol monolayers: the widths  $\delta_s$  and  $\delta_w$  of the surfactant’s and water’s scattering density distributions. As correctly observed by the authors, these thicknesses have a significant contribution from the thermal capillary waves on the studied surface. Li et al. made an attempt to correct for the thermal roughness  $\delta_T$  using for it the formula  $\delta_T = \text{constant}/\sigma^{1/2}$ . Unfortunately, this equation is valid for surfaces of pure liquids only, and is not applicable for surfaces with surfactants – surfactants are known to immobilize the liquid surfaces through the Marangoni effect and, in result, strongly damp the capillary waves [72,73]. The assumption  $\delta_T = \text{constant}/\sigma^{1/2}$  leads to the opposite conclusion – that the higher the surfactant adsorption, the larger the amplitude of the capillary waves; therefore, the thermal roughness estimate from Ref. [70] is overestimated significantly. Moreover, the normal surface dipole affects the amplitude of the short capillary waves [74], and the alcohols alter the surface dipole drastically, changing even its sign [47]. A third complication is that the amplitude of the capillary waves decreases with the distance from the surface (especially for short waves [73]), which complicates additionally the interpretation of  $\delta_s$  and  $\delta_w$  that strictly refer to locations below the surface. In principle, the presented equation of state, in combination with the available theory of the amplitude of the capillary waves [72,74], should allow the accurate prediction of the thermal roughness, but this

is outside the scope of the current work, so we will abstain from discussion of the widths  $\delta_s$  and  $\delta_w$ .

The conclusions from this section have to be viewed with caution, considering the strong approximations behind our model. In particular, the value  $\psi_{w0} = 0.77$  obtained from the tensiometric data for alcohols is too high, which means that the values of  $\Delta z^S$  in Table 2 are more negative than they probably are in reality, especially at low surfactant surface density  $\Gamma_s$ . Therefore, it is quite likely that the observed increase of  $\delta_{sw}$  is actually due to a combination of solvent being expelled from the surface layer and a change in the hydrocarbon chain tilt. However, what is important is that (i) it is clear from the  $\Delta z^S$  values in Table 2 that the squeezing of solvent out of the monolayer has a large contribution to the observed change in the separation  $\delta_{sw}$ , and (ii) there is no apparent disagreement between our model and the available neutron reflectivity data for alcohols.

It is harder to compare our theory with neutron data for  $C_nH_{2n+1}EO_6$ , as the monolayer approximation does not hold here – the thickness of the  $EO_6$  layer is 10.5 Å [19], which corresponds to 3–4 layers of water; in addition, the ether groups of  $C_nH_{2n+1}EO_6$  can be expected to remain hydrated even near the collapse point, an effect that cannot be accounted for within a hard-disc mixture model. Both effects should lead to higher water content in the  $EO_6$  layer, including in strongly compressed monolayers (where our model predicts  $\psi_w \rightarrow 0$  instead, cf. Fig. 7). The expulsion of water from the monolayer that our model predicts in dense monolayers is evident as a qualitative trend from the available neutron scattering measurements (e.g., fig. 9 in Ref. [75]); quantitatively, however, there is disagreement – the experiment [71,75] indeed shows high water content in the dense monolayer (near the critical micelle concentration), due to the association between water and  $C_nH_{2n+1}EO_6$  [71].

#### 4. Discussion and conclusions

Our work develops, to our knowledge, the first comprehensive delocalized model of adsorption of surfactant at a liquid surface with explicit account for the presence of solvent molecules in the surfactant layer. To do this, we utilized the equation of state of Lebowitz et al. for hard-disc mixtures [30] and the approximation for a surface monolayer [29].

We have shown that the osmotic effect due to the solvent molecules corresponds to an effective cohesion in the monolayer, characterized by an osmotic (2D-depletion) lateral attraction parameter  $\beta_{osm}$ . This  $\beta_{osm}$  has been explicitly related to the density  $\psi_{w0}$  of the surface layer of the neat solvent surface and the hard-disc area ratio  $r = \alpha_s/\alpha_w$ , Eq. (16). We have demonstrated that the 1-component sticky disc model with  $\beta$  set to  $\beta_{osm}$  approximates well the more advanced 2-component LHP model, Fig. 3.

We further proposed a formula for the lateral attraction parameter, Eq. (23), that involves the van der Waals attraction between the hydrocarbon chains (the main contribution to  $\beta$ ), the osmotic cohesion effect, and the contribution due to the immersion of the methylene group adjacent to the polar head group. We demonstrated that this formula agrees very well with the surface tension data for three homologous series of surfactants at W|A, Table 1 and Fig. 5.

Our model predicts not only the surfactant adsorption, but also the solvent content in the surface layer, through the solvent's isotherm (13). The solvent is squeezed out of the monolayer as the surfactant adsorption increases (cf. Figs. 2 & 7), which leads to a significant shift in the Gibbs equimolecular surface, Eq. (25). We demonstrated that this shift is largely responsible for the increase with  $\Gamma_s$  of the separation  $\delta_{sw}$  between the centres of the distributions of the scattering densities of the water and the alcohol, which

has been observed in published neutron reflection experiments [70].

The results from our work explain several experimental observations that are puzzling otherwise:

- (i) the 1-component HFL and SD models were previously found successful in describing the adsorption behaviour of numerous surfactants at W|A interface [24], despite the fact that they neglect the solvent molecules. The explanation is the partial cancelation of the osmotic cohesion effect from the solvent and the effect from the immersion in the aqueous phase of the  $CH_2$  group adjacent to the polar head-group, cf. Section 3.
- (ii) An interesting prediction from the model is that, if the chemical potential of water is decreased via addition of surface-inactive electrolyte, this will result in smaller  $\psi_{w0}$  and, as a consequence, in smaller osmotic attraction. Indeed, the monolayer cohesion has been observed to decrease at concentration of NaF or NaCl of the order of 1 M and more (e.g., Fig. 5 in Ref. [47]). However, this effect is complicated by the direct screening of the van der Waals attraction between the hydrocarbon tails by the salt.
- (iii) The small  $n$ -independent lateral attraction parameter found previously for acids and alcohols adsorbed at water|oil interfaces (table 2 in Ref. [24]) is most probably also of osmotic origin.

With regard to the last point, it is not clear how two solvents in two surface layers (one in the aqueous and another in the oil phase) would contribute to the adsorption at water|oil interfaces. Nevertheless, our results predict an interesting dependence of the lateral attraction parameter on the size of the oil molecules: according to Eq. (16), large solvent molecules must lead to large depletion attraction (large  $\beta_{osm}$ ). We hope we will be able to test this prediction in future.

#### Acknowledgements

The funding and technical support from BP through the BP International Centre for Advanced Materials (BP-ICAM) made this research possible and is gratefully acknowledged. Discussions with Prof. Stuart Clarke have helped us to improve this work significantly.

#### References

- [1] A.N. Frumkin (editor), The Basic Problems in Modern Theoretical Electrochemistry: Works from the 14th Meeting of the International Committee of Electrochemical Thermodynamics and Kinetics. Mir; 1965, in Russian
- [2] F.P. Buff, F.H. Stillinger, Statistical mechanical theory of double-layer structure and properties, J. Phys. Chem. 39 (1963) 1911.
- [3] R. Parsons, J. Electroanal. Chem. 7 (1964) 136–152.
- [4] F.P. Buff, F.H. Stillinger, in: A.N. Frumkin (Ed.), Basic Problems of Modern Theoretical Electrochemistry, Mir, in Russian, 1965.
- [5] E. Helfand, H.L. Frisch, J.L. Lebowitz, J. Chem. Phys. 34 (1961) 1037.
- [6] A.N. Frumkin, J. Electroanal. Chem. 7 (1964) 152–155.
- [7] R. Parsons, Russ. J. Electrochem. 37 (2001) 647–652.
- [8] R. Parsons, J. Electroanal. Chem. 8 (1964) 93–98.
- [9] V.B. Fainerman, R. Miller, E.V. Aksenenko, A.V. Makievski, in: V.B. Fainerman, D. Möbius, R. Miller (Eds.), Surfactants – Chemistry, Interfacial Properties, Applications, Elsevier, 2001 (Chapter 3).
- [10] K. Lunkenheimer, W. Barzyk, R. Hirte, R. Rudert, Langmuir 19 (2003) 6140.
- [11] J. Lucassen, D. Giles, J. Chem. Soc., Faraday Trans. 171 (1975) 217–232.
- [12] S.-Y. Lin, Y.-C. Lee, M.-W. Yang, H.-S. Liu, Langmuir 19 (2003) 3164–3171.
- [13] M. Lj, D.M. Dražić Vračar, Corrosion Science 44 (2002) 1669–1680.
- [14] V.S. Markin, M.I. Volkova-Gugeshashvili, A.G. Volkov, J. Phys. Chem. B 110 (2006) 11415–11420.
- [15] C.E. Morgan, C.J.W. Breward, I.M. Griffiths, P.D. Howell, J. Penfold, R.K. Thomas, I. Tucker, J.T. Petkov, J.R.P. Webster, Langmuir 28 (2012) 17339–17348.

- [16] J. Lawrence, R. Parsons, *J. Phys. Chem.* 73 (1969) 3577.
- [17] T. Smith, *J. Colloid Interface Sci.* 23 (1967) 27.
- [18] D.K. Chattoraj, K.S. Birdi, *Adsorption and the Gibbs Surface Excess*, Plenum Press, 1984. Chapters 5&6.
- [19] Y.J. Nikas, S. Puvvada, D. Blankschtein, *Langmuir* 8 (1992) 2680–2689.
- [20] I.B. Ivanov, K.P. Ananthapadmanabhan, A. Lips, *Adv. Colloid Interface Sci.* 123–126 (2006) 189.
- [21] T.D. Gurkov, I.B. Ivanov, in: *Proc. 4th World Congress on Emulsions*, Lyon, 2006, p. 509.
- [22] I.B. Ivanov, K.D. Danov, D. Dimitrova, M. Boyanov, K.P. Ananthapadmanabhan, A. Lips, *Colloids Surfaces A* 354 (2010) 118.
- [23] R.I. Slavchov, S.I. Karakashev, I.B. Ivanov, in: L. Römsted (Ed.), *Surfactant Science and Technology: Retrospects and Prospects*, Taylor and Francis, LLC, 2014 (Chapter 2).
- [24] R.I. Slavchov, I.B. Ivanov, *Soft Matter* 13 (2017) 8829–8848.
- [25] A. Frumkin, *Z. Phys. Chem.* 116 (1925) 466.
- [26] T. Söderlund, J.-M.I. Alakoskela, A.L. Pakkanen, P.K.J. Kinnunen, *Biophys. J.* 85 (2003) 2333–2341.
- [27] L. Salem, *J. Chem. Phys.* 37 (1962) 2100–2113.
- [28] J.N. Israelachvili, *Intermolecular and Surface Forces*, 3rd ed., Academic Press, 2011.
- [29] R. Defay, I. Prigogine, *Surface Tension and Adsorption*, Longmans, 1966.
- [30] J.L. Lebowitz, E. Helfand, E. Praestgaard, *J. Chem. Phys.* 43 (1965) 774.
- [31] D.P. Fraser, M.J. Zuckermann, O.G. Mouritsen, *Phys. Rev. A* 43 (1991) 6642.
- [32] M. Mezger, F. Sedlmeier, D. Horinek, H. Reichert, D. Pontoni, H. Dosch, *J. Am. Chem. Soc.* 132 (2010) 6735.
- [33] Analogous to the virial expansion of the 3D osmotic pressure: T.L. Hill, *An Introduction to Statistical Thermodynamics*, Addison-Wesley, 1962 (sec. 19-1).
- [34] P. Attard, *J. Chem. Phys.* 91 (1989) 3083.
- [35] L.R. Pratt, F. Chandler, *J. Chem. Phys.* 67 (1977) 3683.
- [36] E.H. Lucassen-Reynders, M. van den Tempel, *Proc. IVth Int. Cong. Surface Active Substances*, vol. 2, Brussels, 1964, p. 779.
- [37] M.A. Volmer, P. Mahnert, *Z. Phys. Chem.* 115 (1925) 236.
- [38] J.H. De Boer, *The Dynamical Character of Adsorption*, Clarendon Press, 1953.
- [39] C. Tanford, *The Hydrophobic Effect*, Wiley, 1980.
- [40] P. Kruglyakov, *Hydrophile-Lipophile Balance of Surfactants and Solid Particles*, Elsevier, 2000.
- [41] R.A. Pierotti, *Chem. Rev.* 76 (1976) 717–726.
- [42] R.I. Slavchov, I.M. Dimitrova, T. Ivanov, *J. Chem. Phys.* 143 (2015) 154707.
- [43] R.I. Slavchov, I.M. Dimitrova, I.B. Ivanov, in: R.G. Rubio, Y.S. Ryazantsev, V.M. Starov, G.X. Huang, A.P. Chetverikov, P. Arena, A.A. Nepomnyashchy, A. Ferrús, E.G. Morozov (Eds.), *Without Bounds: a Scientific Canvas of Nonlinearity and Complex Dynamics*, Springer-Verlag, 2013, p. 199.
- [44] W. Hüchel, *Theoretical Principles of Organic Chemistry*, vol. II, Elsevier, 1958, p. 435.
- [45] A.I. Kitaigorodskii, *Organic Chemical Crystallography*, Consultant Bureau, 1961.
- [46] A. Gericke, J. Simon-Kutscher, H. Hühnerfuss, *Langmuir* 9 (1993) 3115–3121.
- [47] R.V. Peshkova, I.L. Minkov, R. Tsekov, R.I. Slavchov, *Langmuir* 32 (2016) 8858–8871.
- [48] I. Langmuir, *J. Chem. Phys.* 1 (1933) 756.
- [49] G. Jura, W.D. Harkins, *J. Chem. Phys.* 12 (1944) 113.
- [50] N.K. Adam, *The Physics and Chemistry of Surfaces*, Clarendon Press, 1941.
- [51] A.D. Bond, *New J. Chem.* 28 (2004) 104–114.
- [52] H. Lange, P. Jeschke, in: M.J. Schick (Ed.), *Nonionic Surfactants. Physical Chemistry*, Marcel Dekker Inc., New York, 1987.
- [53] J.T. Davies, E. Rideal, *Interfacial Phenomena*, Academic Press, 1963 (Chapters 4&5).
- [54] K.D. Danov, P.A. Kralchevsky, K.P. Ananthapadmanabhan, A. Lips, *J. Colloid Interface Sci.* 300 (2006) 809.
- [55] A.J. Kumpulainen, C.M. Persson, J.C. Eriksson, E.C. Tyrode, C.M. Johnson, *Langmuir* 21 (2005) 305.
- [56] J.R. Hommelen, *J. Colloid Science* 14 (1959) 385.
- [57] S.Y. Lin, K. McKeigue, C. Maldarelli, *Langmuir* 7 (1991) 1055.
- [58] S.Y. Lin, T.L. Lu, W.B. Hwang, *Langmuir* 10 (1994) 3442.
- [59] R. Vochten, G. Petre, *J. Colloid Interface Sci.* 42 (1973) 320.
- [60] V.B. Fainerman, S.V. Lylyk, *Koll. Zh.* 45 (1983) 500.
- [61] C.C. Addison, *J. Chem. Soc.* (1945) 98.
- [62] M. Aratono, S. Uryu, Y. Hayami, K. Motomura, R. Matuura, *J. Colloid Interface Sci.* 98 (1984) 33.
- [63] W. Barzyk, K. Lunkenheimer, P. Warszyński, B. Jachimska, A. Pomianowski, *Colloids Surf. A* 443 (2014) 515–524.
- [64] R. Wüstneck, R. Miller, *Colloids Surf.* 47 (1990) 15.
- [65] K. Lunkenheimer, R. Hirte, *J. Phys. Chem.* 96 (1992) 8683.
- [66] V.D. Dolzhikova, Y.V. Goryunov, B.D. Summ, *Colloid J.* 44 (1982) 560.
- [67] K. Malysa, R. Miller, K. Lunkenheimer, *Colloids Surf.* 53 (1991) 47.
- [68] F. Suarez, C.M. Romero, *J. Chem. Eng. Data* 56 (2011) 1778–1786.
- [69] N. Nishikido, T. Takahara, H. Kobayashi, M. Tanaka, *Bull. Chem. Soc. Jpn.* 55 (1982) 3085–3088.
- [70] Z.X. Li, J.R. Lu, R.K. Thomas, A.R. Rennie, J. Penfold, *J. Chem. Soc., Faraday Trans.* 92 (1996) 565–572.
- [71] J.R. Lu, Z.X. Li, R.K. Thomas, E.J. Stalpes, I. Tucker, *J. Phys. Chem.* 97 (1993) 8012–8020.
- [72] J. Daillant, L. Bosio, J.J. Benattar, J. Meunier, *Europhys. Lett.* 8 (1989) 453–458.
- [73] V.G. Levich, *Physicochemical hydrodynamics*. Gosudarstvennoe izdatel'stvo fiziko-matematicheskoy literatury, Moscow; 1959 (in Russian); Englewood Cliffs, NJ., Prentice-Hall; 1962 (in English). Sec. XI
- [74] R. Tsekov, H.J. Schulze, B. Radoev, E. Manev, *Colloids Surf. A* 149 (1999) 475–479.
- [75] J.R. Lu, T.J. Su, Z.X. Li, R.K. Thomas, E.J. Stalpes, I. Tucker, *J. Phys. Chem. B* 101 (1997) 10332–10339.